



POLITECNICO DI TORINO
Repository ISTITUZIONALE

Small scale of subgrid scales in the Large Eddy Simulation of compressible turbulent flows

Original

Small scale of subgrid scales in the Large Eddy Simulation of compressible turbulent flows / TORDELLA D.; IOVIENO M.. - STAMPA. - 17(2005), pp. 210-210 +CD. ((Intervento presentato al convegno AIMETA 2005 tenutosi a Firenze nel 11-15 Settembre 2005.

Availability:

This version is available at: 11583/1542913 since:

Publisher:

Firenze Univeristy Press

Published

DOI:

Terms of use:

openAccess

This article is made available under terms and conditions as specified in the corresponding bibliographic description in the repository

Publisher copyright

(Article begins on next page)

Small scale localization in the simulation of a turbulent jet at $M = 5$

Daniela Tordella, Michele Iovieno

Politecnico di Torino, Dipartimento di Ingegneria Aeronautica e Spaziale

C.so Duca degli Abruzzi 24, 10129 Torino, Italy

E-mail: daniela.tordella@polito.it, michele.iovieno@polito.it

Keywords: turbulence, compressible jets, transition, sub-grid scale model

SUMMARY: It is proposed a methodology for the automatic selective insertion-elimination of subgrid scale stresses in the numerical simulation of transitional laminar-turbulent flows in both compressible and incompressible regimes. By means of a functional of the filtered vorticity field, it is possible to approximatively locate the flow regions that are rich in small scale motions. In these regions, it can be opportune to filter the equations of motion to carry out a Large Eddy Simulation, that is, a simulation where the larger scales only are resolved, but the small scale dynamics is considered and represented through proper terms in the equations. In case of compressible regimes, a functional of the pressure local variation and divergence can be associated to the functional previously mentioned in order to determine the eventual presence of shocks. In such a way, it is possible to locate the regions where, to capture the shock, it is necessary to insert an explicit numerical dissipation and suppress the subgrid model.

1. SMALL SCALE LOCALIZATION CRITERIUM

The large eddy simulation method is going to be one of the more used tools to predict the behaviour of turbulent flows in many different physical and engineering applications. Compressible turbulent flows in nature may be characterized by very high Reynolds numbers. Consequently, any attempt to numerically solve the Navier-Stokes equations for such flows requires a great number of scales to be resolved. At present, the largest three-dimensional turbulence simulations have a resolution that allows a ratio between the largest scales and the smallest scales of no more than one thousand, thus, in general, the large scales only of the flow can accurately be simulated and a large-eddy simulation (LES) approach is necessary.

In this context, there are two conflicting requirements: 1) to capture discontinuities such as shock waves without the introduction of spurious oscillations, which requires a high numerical dissipation, 2) the numerical algorithm should not damp the turbulent structures, which requires a low numerical dissipation. The problem of the reliable representation of the presence of smaller scales in compressible turbulent flow simulations has often been overlooked; it has often been assumed that numerical dissipation, implicit in upwind shock capturing numerical schemes, could simulate net energy transfer from larger to smaller scales. However, this is questionable and moreover it has been shown (Ducros *et al.* [1999]) that such an approach is not compatible with LES modelling due to the antithetic behaviour of the high numerical viscosity which overwhelms the subgrid scale term effects.

Our aim is the development of a method that allows the contemporary detection of strong shocks and small scale turbulence. To locate the small scales we propose a) to introduce a criterium based on the local structure of the vorticity field, in particular on its

three dimensional character and b) to use a centered low dissipation scheme (Ducros *et al.* [1999] and Yee *et al.* [1999]) coupled to a shock sensor function which, in case, activates a local explicit artificial dissipation. In such a way, it is possible to selectively introduce a compressible LES model, for example the angular momentum model (Iovieno and Tordella [2002]).

The criterium for the small scale localization is based on the introduction of the functional

$$f(\langle \mathbf{u} \rangle, \langle \boldsymbol{\omega} \rangle) = \frac{|\langle \boldsymbol{\omega} \rangle \cdot \nabla \langle \mathbf{u} \rangle|}{|\langle \boldsymbol{\omega} \rangle|^2} \quad (1)$$

which uses information from just one filtering level, Δ , and where $\langle \mathbf{u} \rangle, \langle \boldsymbol{\omega} \rangle$ are the filtered velocity and vorticity fields, respectively. The behaviour of f is observed in a developed HI turbulence field, either fully resolved (DNS) or under-resolved (LES, with various filter scale). At this point, a range of f values typical for HIT can be selected by means of the insertion of a threshold t_ω and the computation of the probability density distribution that f be larger than the given threshold. The value of this threshold t_ω was determined through *a priori* tests on high-resolution, direct numerical simulation of incompressible homogeneous and isotropic turbulence (Biferale *et al.* [2005]) with $Re_\lambda = 280$.

In this work, the criterium $-f \geq t_\omega$ was applied to snapshots from a numerical simulation of the temporal decay of a hypersonic jet with Mach number of 5 (Rossi *et al.* [1997]). This has made it possible to identify the presence of small scale and then the region where it is opportune to locally modify the motion equations filtering them and inserting a subgrid scale turbulence model (Iovieno and Tordella, 2002). In such a way the Reynolds stress balance is corrected by adding the contribution coming from the subgrid term to the turbulent stresses, which improves the general properties of the temporal and spatial evolution of the simulated field.

2. DESCRIPTION OF THE TEST FLOW

In fig. 1, a visualization of the instantaneous vorticity field of the jet in a section placed 6 diameter downstream of the inlet at nearly 13 time scales from the initial instant and, in fig.2, the representation of the averaged radial and axial distributions of the streamwise velocity component. In this simulation the hydrodynamical equations are integrated numerically using a three-dimensional version of the Piecewise Parabolic Method code (Colella and Woodward 1984). The domain is $(0, 10\pi a) \times (-6.7a, 6.7a) \times (-6.7a, 6.7a)$, where a is the initial jet radius, is described by a Cartesian coordinate system (x, y, z) and is covered by a $128 \times 128 \times 128$ and a $256 \times 256 \times 256$ grids. The initial flow structure is a cylindrical jet, with its symmetry axis lying along the x -direction, which is also the direction of the initial jet velocity. The interface between the initial jet and the surrounding fluid is a smoothly varying (hyperbolic secant) velocity shear layer. The boundary conditions are free outflow conditions at the upper and lower boundaries in the y and z directions. The boundary conditions along x direction are periodic, see Rossi *et al.* (1997), Bodo *et al.* (1998).

3. A PRIORI TESTS

3.1 On Homogeneous Isotropic Turbulence in a box

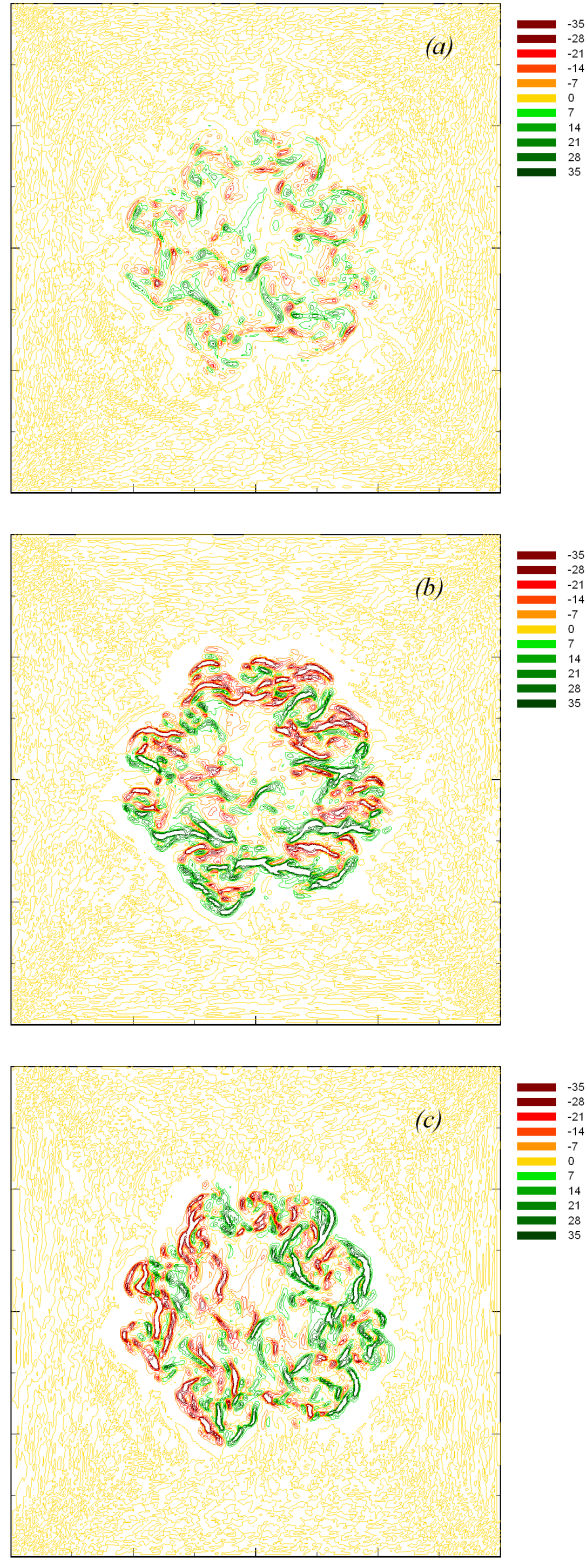


Figure 1: Contour plot of the vorticity components, (a) w_x , (b) w_y , (c) w_z .

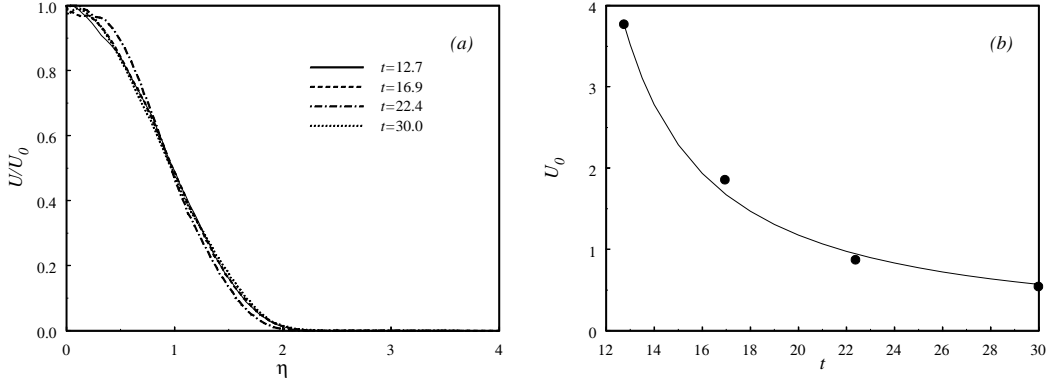


Figure 2: Radial (a) and axial (b) distributions of the mean velocity.

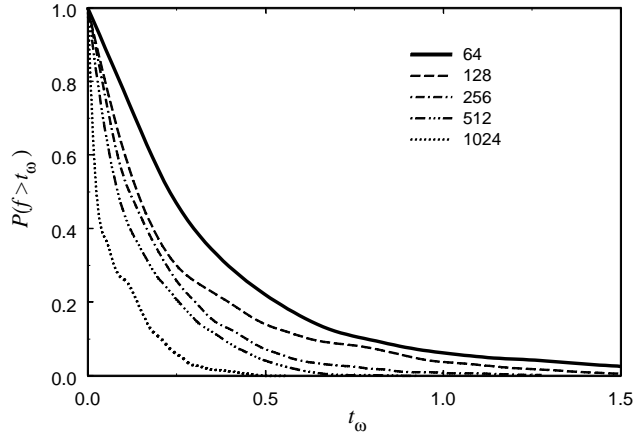


Figure 3: Distribution of f on different resolutions for homogeneous and isotropic turbulence.

A priori tests on a DNS of homogeneous and isotropic (incompressible) turbulence (1024^3 grid, see Biferale et al. 2005) and on filtered fields ($64^3, 128^3, 256^3, 512^3$) deduced from this DNS have been carried out. The 1024^3 turbulence is here considered a resolved fully developed turbulent field and is taken as reference. The functional f is computed in all these fields. As previously pointed out, the range of the f possible values in a resolved HIT and in under-resolved HIT can be obtained by considering a threshold t_ω and by computing the probability density distribution that f is larger than the a given threshold value, see fig.3. In this figure it can be noticed that, in the resolved turbulence, there is practically zero probability of having $f > 0.5$. However, in the unresolved cases, larger values are possible. Thus, if in a simulation of a fully developed turbulent flow, f assumes values larger than 0.5, the turbulent field is probably under-resolved and can thus benefit from the activation of a local LES (by inserting a sub-grid scale term in the motion equation). Figure 3 shows also that in the under-resolved fields, values lower than 0.5 – for example values in the range

$[0.2, 0.5]$ – have a much greater probability to exist than in the resolved field. This difference is then shrinking getting close to $f = 0$. So, it can be argued that also when f is in the $[0.2, 0.5]$ range, there is a definite chance to improve the simulation by switching to a local LES.

3.1 On the time evolution of a turbulent jet at $M=5$

Figure 4 shows the contour lines of the functional f computed in the central section of the jet (with respect to the computational domain, $x = 5\pi a$). Island of high f values can be observed. According to the criterium above, these islands can be viewed as regions where small scales are present and are under-resolved. By varying the threshold t_ω , maps of regions where $f \geq t_\omega$ can be obtained. For instance, figure 5 describes the distribution of such regions in the mid-section of the jet ($x = \pi a, t = 13$ initial time scales). Two values of $t_\omega = 0.3$ and $t_\omega = 0.5$ are compared. It is observed that, by increasing t_ω , the global area occupied by the small scales at a given time instant is reduced.

At this point it is necessary to calibrate the t_ω value with information coming from laboratory experiments or from highly resolved numerical simulation of a jet at Mach 5. This last information is not available at the current state of the art. Data from a few experiments on compressible jets up to Mach 4 are instead available. In particular, the spatial growth rate as a function of the global Mach number for experiments on jets or on plane mixing layers were collected in the famous "Langley curve", see e.g. Smits and Dussage (1996, cf. par. 6.3, fig. 6.2). In the present test, recalling that the spatial evolution is suppressed due to the periodic b.c.s, we can estimate the spatial spreading rate by applying the Taylor's transformation and by computing the temporal spreading, $d\delta(t)/dt$, of the simulated jet

$$\frac{d\delta}{dx} = \frac{d\delta}{dt} \frac{dt}{dx} = \frac{1}{U_0} \frac{dt}{dx} \quad (2)$$

where $U_0 = U_0(t)$ is the averaged axial velocity.

In the temporal decay of this jet, for $t > 10$, we can reasonably assume to have reached near similarity conditions. This implies that the filtered transversal distribution of the streamwise velocity is of the kind $U = U_0(t)f(\eta)$, where η is the lateral coordinate normalized with the thickness $\delta(t)$. Due to symmetry reasons, y and z play the same role, thus, for the turbulent stresses we can put $\tau_{xy} = \tau_{xz} = \tau$. Furthermore, the streamwise momentum balance for the filtered field yields

$$\frac{\partial U}{\partial t} = \frac{\partial \tau}{\partial y} + \frac{\partial \tau}{\partial z} + \frac{\partial \tau^{sgs}}{\partial y} + \frac{\partial \tau^{sgs}}{\partial z} \quad (3)$$

By assuming the similarity transformation for the turbulent stresses, $\tau = \tau_0(t)g(\eta)$ and $\tau^{sgs} = \tau_0^{sgs}(t)g^{sgs}(\eta)$ – where the suffix *sgs* means sub-grid scale, and τ_0 and τ_0^{sgs} are the reference values for the resolved and the sub-grid scale stress distributions (maximum values) – and by inserting the similarity transformation in (3), it is possible to deduce that the temporal spreading is proportional to the stress modified by the sub-grid contribution

$$\frac{d\delta}{dt} = \left(\frac{d\delta}{dt}\right)_{nc} \frac{\tau_0 + \tau_0^{sgs}}{\tau_0} \quad (4)$$

where index *nc* (non corrected) indicates the spreading obtained from the simulation before the insertion of the sub-grid terms. Now, the subgrid scale contribution to the turbulent

stress, that is shown in figure 6a, depends on the value of t_ω . From (2) and (4), it is possible to estimate the correction to the spreading rate due to the setting off of the sub-grid terms in the simulation. We have here used the Intrinsic Angular Momentum Model (Iovieno and Tordella, 2002), which is a differential model suitable to highly dishomogeneous turbulent fields. Figure 6b shows the correction obtained varying t_ω and varying the simulation resolution. It is observed that the corrected values of the spatial spreading rate are closer to the value extrapolated from the "Langley curve", at Mach 5, than the original raw data and that the improvement is higher if the resolution of the simulation is lower.

4. FINAL COMMENTS

As far as the shock localization is concerned, a sensor can be conceived for example in the form of a function

$$s = \alpha\beta, \quad \alpha = \frac{(\nabla \cdot \langle \mathbf{u} \rangle)^2}{(\nabla \cdot \langle \mathbf{u} \rangle)^2 + \langle \omega \rangle^2}, \quad \beta = \left| \frac{\langle p \rangle_{j+1} - 2\langle p \rangle_j + \langle p \rangle_{j-1}}{\langle p \rangle_{j+1} + 2\langle p \rangle_j + \langle p \rangle_{j-1}} \right| \quad (5)$$

that should multiply the explicit artificial dissipation terms in the discretized balance equations (Ducros et al. 1999). The identification of the regions where the shocks are present will then coincide with the setting off of the numerical artificial dissipation.

By coupling the method of small scales localization here described to the above procedure of shocks localization, a description of the interaction between shocks and large-scale turbulence structures can be obtained. Furthermore, sensors (1) and (5) are not limited by the mesh structure and could be of help to obtain a dynamic adaptation of the mesh to the flow. The implementation of sensors that are able to effectively detect subgrid scales and shocks would enable accurate LES of complex flows to be obtained without any a priori assumption on the flow structure. The local character of such functionals should allow easy parallelization.

REFERENCES

- Biferale L., Boffetta G., Celani A., Lanotte A., Toschi F. (2005), "Particle trapping in three-dimensional fully developed turbulence", *Phys. Fluids*. **17**(2), 021701/1-4
- Bodo G., Rossi P., Massaglia S., (1998), "Three-dimensional simulations of jets", *Ast. & Astr.* **333**, pagg. 1117.
- Colella P., Woodward P.R., (1984), "The piecewise parabolic method (ppm) for gas-dynamical simulations", *J.Comp. Phys.* **54**, pagg. 174-201.
- Ducros F., Ferrand V., Nicoud F., Weber C., Darracq D., Gacherieu C., Poinot T. (1999), "Large-eddy simulation of the shock-turbulence interaction", *J.Comp. Phys.* **152**, pagg. 517-549.
- Iovieno M., Tordella D. (2002), "The angular momentum equation for a finite element of fluid: a new representation and application to turbulent flows", *Phys. Fluids* **14**,(8), 2673-2682.
- Rossi P., Bodo G., Massaglia S., Ferrari A. (1997), "Evolution of Kelvin-Helmholtz instabilities in radiative jets: shock structures and entrainment properties", *Ast. & Astr.* **321**, pagg. 672-684.
- Smits J., Dussage JP (1996), *Turbulent shear layers in supersonic flow*, AIP Press, Woodbury, New York.
- Yee H.C., Sandham N.D., Djomehri M.J. (1999), "Low-dissipative high-order shock-capturing methods using characteristic-based filters", *J. Comp. Phys.* **150**, pagg. 199-238.

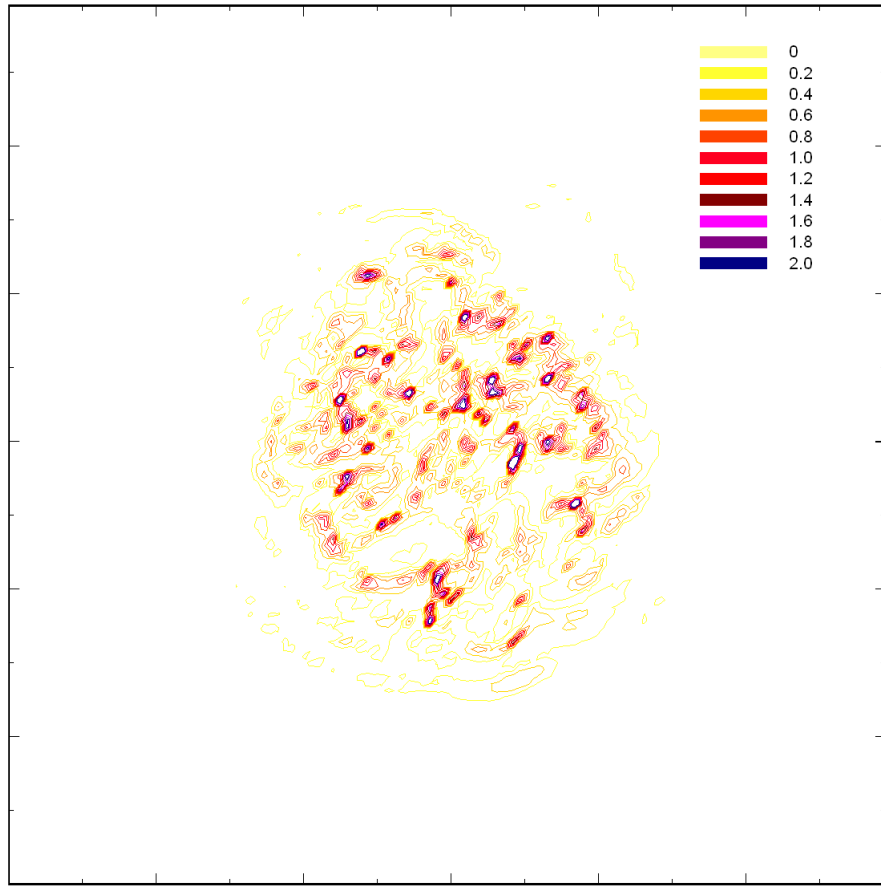


Figure 4: Contour plot of the functional f given by equation (1), $x = 5\pi a, t = 13$ time units.

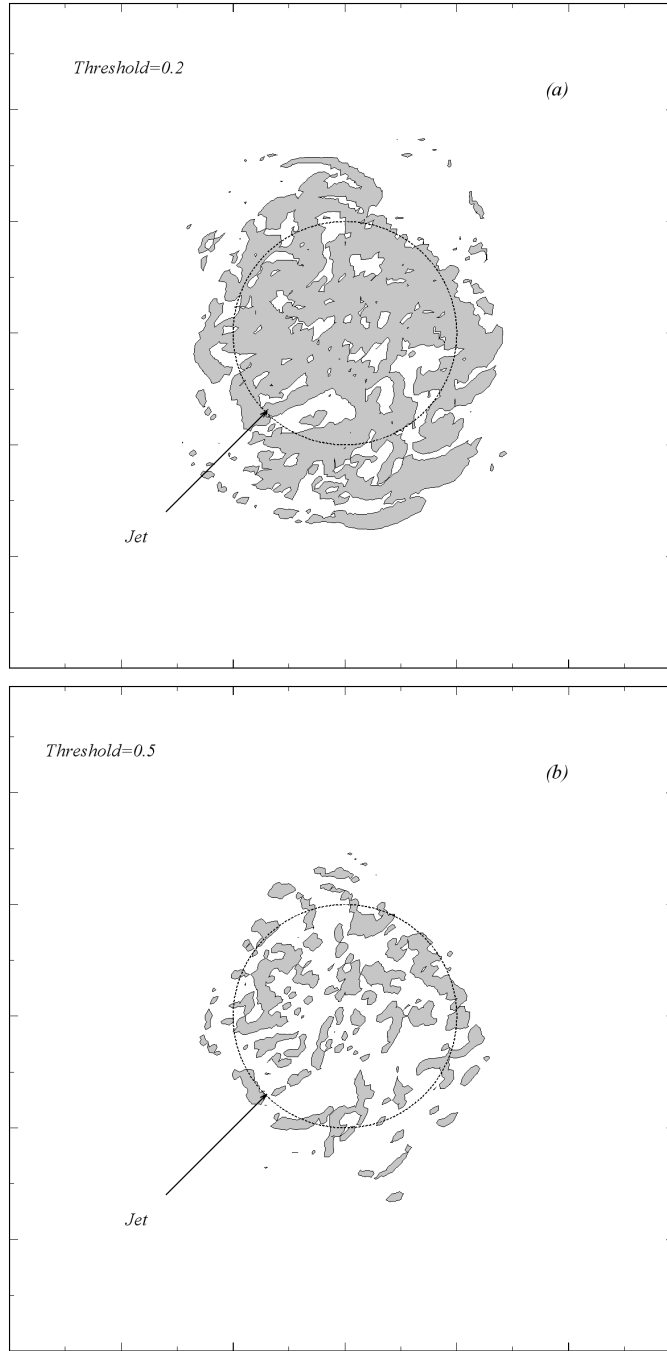


Figure 5: Visualization of the regions where subfilter scales are present according to a selected threshold t_ω on the functional f : (a) $t_\omega = 0.2$, (b) $t_\omega = 0.5$

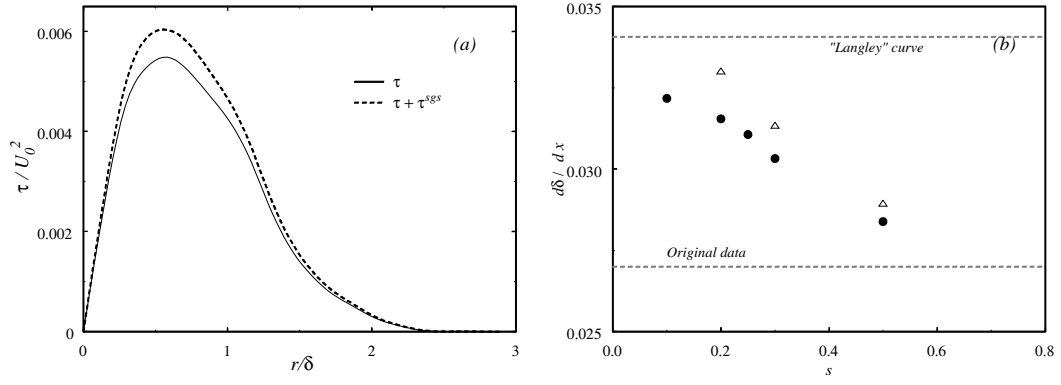


Figure 6: (a) Transversal distributions of the Reynolds stress, without and with the subgrid scale contribution, (b) Dependence of the correction on the spatial growth rate on t_ω , two different resolutions: circles 256^3 , triangles 128^3 . For "Langley curve" data see Smits and Dussauge (1996).